J Herbmed Pharmacol. 2026; 15(3): 333-344.

http://www.herbmedpharmacol.com doi: 10.34172/jhp.53476

Journal of Herbmed Pharmacology

In silico molecular docking study of flavanols methyl ethers from *Alpinia monopleura* as potential inhibitors of inflammatory targets

Agung Wibawa Mahatva Yodha[1*], Reymon[1], Nirwati Rusli[1], Musdalipah[1], Angriani Fusvita[2], Wahyuni[3], Arfan[3], Sahidin[3]

[1]D3 Pharmacy Study Program, Politeknik Bina Husada Kendari, Indonesia
[2]D4 Medical Laboratory Technology Study Program, Politeknik Bina Husada Kendari, Indonesia
[3]Pharmacy Study Program, Faculty of Pharmacy, University of Halu Oleo Kendari, Indonesia

ARTICLE INFO

Article Type:
Original Article

Article History:
Received: 21 Oct. 2025
Revised: 22 Apr. 2026
Accepted: 23 Apr. 2026
Epublished: 1 Jul. 2026

Keywords:
Flavonoid
Molecular docking
Structure activity relationship
Protein binding
Inflammation mediators

ABSTRACT

Introduction: Inflammation plays a central role in various chronic diseases. Flavonoids are widely recognized for their pharmacological potential, including anti-inflammatory properties. This study aimed to isolate O-methylated flavonols from *Alpinia monopleura* and to predict their potential anti-inflammatory activity using computational approaches.

Methods: Rhizomes of *A. monopleura* were extracted with methanol, partitioned, and fractionated by vacuum liquid chromatography (VLC). Isolated compounds were characterized by ^{1}H- and ^{13}C-NMR spectroscopy. The anti-inflammatory potential was evaluated by molecular docking against multiple inflammation-related targets using AutoDock Vina, with native ligands as references, followed by in silico pharmacokinetic and toxicity predictions using pkCSM and ProTox 3.0.

Results: Two O-methylated flavonols, kaempferol 3,7,4′-trimethyl ether (2a) and quercetin 3,7,4′-trimethyl ether (2b), were isolated from the ethyl acetate fraction of *A. monopleura*. Both compounds exhibited favorable binding energies toward multiple inflammatory targets. Compounds 2a and 2b showed stronger binding than native ligands against inducible nitric oxide synthase (iNOS), lipoxygenase (LOX), and mPGES-1, and interacted with COX-2, IKK, JAK2, and NOX5, which are key proteins regulating inflammatory signaling pathways, with binding energies generally below −8.0 kcal/mol. Predicted pharmacokinetic profiles indicated good intestinal absorption and membrane permeability, with acceptable toxicity, with binding energies generally below −8.0 kcal/mol. Predicted pharmacokinetic profiles indicated good intestinal absorption and membrane permeability, with acceptable toxicity.

Conclusion: O-methylated flavonols from *A. monopleura* showed potential as multi-target anti-inflammatory leads based on in silico analyses. These findings provide a scientific basis for further experimental studies and support the exploration of *A. monopleura*–derived flavonols as candidate compounds for the development of safer anti-inflammatory agents. Future in vitro and in vivo studies are warranted to validate their pharmacological efficacy and relevance to clinical practice.

Implication for health policy/practice/research/medical education:
O-methylated flavonols from *Alpinia monopleura* have the potential to serve as safer multi-target anti-inflammatory agents, thereby supporting the development of natural product–based research and enriching healthcare practice in the advancement of evidence-based anti-inflammatory therapies.

Please cite this paper as: Yodha AWM, Reymon, Rusli N, Musdalipah, Fusvita A, Wahyuni, et al. In silico molecular docking study of flavanols methyl ethers from *Alpinia monopleura* as potential inhibitors of inflammatory targets. J Herbmed Pharmacol. 2026;15(3):333-344. doi: 10.34172/jhp.53476.

***Corresponding author**: Agung Wibawa Mahatva Yodha,
Email: yodhaagung@gmail.com

Introduction

Chronic inflammation plays a pivotal role in the pathogenesis of various degenerative and metabolic diseases, including arthritis, cardiovascular disorders, and neurodegenerative conditions (1-3). Therefore, the search for novel anti-inflammatory agents with effective activity and favorable toxicity profiles remains a priority in pharmaceutical and medicinal chemistry research. Flavanols such as kaempferol and quercetin have long been recognized for their antioxidant properties and their ability to modulate key inflammatory mediators, including the enzymes cyclooxygenase (COX), lipoxygenase (LOX), and inducible nitric oxide synthase (iNOS), as well as the transcription factor nuclear factor kappa B (NF-κB), which regulates the expression of multiple pro-inflammatory genes. Consequently, their derivatives, particularly methylated compounds at phenolic positions, have emerged as attractive targets for pharmacological and mechanistic studies (4-7).

The Zingiberaceae family represents an important source of bioactive compounds with anti-inflammatory potential (8,9). Several members of the genera *Alpinia* and *Etlingera* have been reported to exhibit anti-inflammatory effects in both in vitro and in vivo assays, largely attributed to their diverse mixtures of flavonoids, diarylheptanoids, phenolics, and essential oils (10-14). Recent review articles have highlighted the activity of numerous *Alpinia* species against inflammatory mediators, positioning this genus as a promising candidate for the discovery of novel anti-inflammatory molecules (15).

Alpinia monopleura is a Zingiberaceae species native to eastern Indonesia and is relatively less documented than its close relatives. Preliminary studies on this species have reported its secondary metabolite profile and biological activities, including antioxidant and antibacterial effects from its extracts and essential oils, reinforcing its pharmacological potential as a source of bioactive compounds (13,16). Furthermore, extracts and fractions have also demonstrated potential anticancer and anti-inflammatory activities (13,17). The anti-inflammatory potential has been attributed to strong interactions with COX-2 by compounds such as 3′,5-dihydroxy-7,4′-dimethoxyflavone and 5-hydro-7,8,2′-trimethoxyflavanone, which effectively reduce inflammation. These findings provide a solid foundation for the isolation and characterization of minor compounds, including flavanols methyl ethers, and for further evaluation of their anti-inflammatory activities.

Methylation of phenolic groups in flavonoids enhances lipophilicity and metabolic stability, thereby improving bioavailability and prolonging residence time in circulation (18). This modification simultaneously reduces the proton-donating capacity of phenolic groups and hydrogen bond formation, which may alter flavonoid affinity patterns toward their targets (19). Its impact on enzymes and anti-inflammatory pathways such as COX, LOX, mPGES-1, iNOS, and NF-κB/JAK is structurally specific (20-23). However, despite increasing reports on methylated flavonoids, systematic information regarding the target selectivity and binding behavior of flavonol methyl ethers, particularly those derived from underexplored *Alpinia* species, remains limited. Therefore, a comprehensive study using in silico approaches is highly relevant to elucidate the mechanisms of action and prioritize the most susceptible targets for these compounds.

To date, no study has specifically reported the isolation and structure-based in silico evaluation of flavonol methyl ethers from *A. monopleura* in relation to key inflammatory signaling targets. Most previous studies have focused on crude extracts, major constituents, or biological screening without providing molecular-level insight into ligand–target interactions or target prioritization. This gap limits mechanistic understanding and rational lead identification for anti-inflammatory drug discovery from this species.

Based on this research gap, the present study aims to isolate flavonol methyl ethers from *A. monopleura*, elucidate their chemical structures, and systematically evaluate their interactions with multiple inflammation-related protein targets using molecular docking and computational analysis. The novelty of this work lies in the first report of flavanols methyl ethers from *A. monopleura* combined with a structure-based in silico assessment to identify their most promising anti-inflammatory targets. The findings are expected to provide preliminary molecular evidence supporting the potential of these compounds as early-stage lead candidates and to guide future experimental validation in vitro.

Material and Methods

Sample preparation and extraction

The rhizomes of *A. monopleura* were collected from Southeast Sulawesi and botanically identified at the Herbarium of the Faculty of Pharmacy, Halu Oleo University (Voucher No. 179/UN29.18/PP/2025). The plant material was thoroughly washed, dried at a temperature not exceeding 40 °C until constant weight was reached, and ground into fine powder (mesh size 40–60). A total of 500 g of the dried powder was extracted with 80% methanol (MeOH:H_2O, v/v) using maceration at room temperature for three consecutive 24-hour periods. The combined filtrates were concentrated under reduced pressure at ≤40 °C to obtain a viscous extract (13,24).

Fractionation and purification

The methanol extract was partitioned with n-hexane to remove non-polar compounds, followed by extraction with ethyl acetate (3 × 300 mL). The resulting ethyl acetate fraction was evaporated to dryness (25,26). This semi-polar fraction was subsequently fractionated using vacuum liquid chromatography (VLC) on silica

gel 60 GF254 with a sample-to-silica ratio of 1:30 and a gradient system of n-hexane: ethyl acetate (9:1, 8:2, 7:3, 5:5) and ethyl acetate: methanol (8:2). The obtained fractions were monitored by thin layer chromatography (TLC) using n-hexane: ethyl acetate (9:1) as the solvent system. Visualization was performed under UV 254 nm and by spraying with $CeSO_4$–H_2SO_4 reagent. Fractions with similar chromatographic profiles were pooled for subsequent purification (17).

Further purification was carried out using radial chromatography on silica gel 60 GF254 containing gypsum with n-hexane: ethyl acetate (7:3), followed by 100% ethyl acetate as eluents. The fractions obtained from radial chromatography were monitored by TLC until a single band was achieved (10).

Structure elucidation

The purified isolate (± 8–10 mg) was dissolved in 0.6 mL of deuterated solvent $CDCl_3$ and transferred into a 5 mm NMR tube. Spectra were recorded on a Jeol JNM-ECS400 spectrometer operating at 400 MHz for ^1H and 100 MHz for ^{13}C at 25 °C. Chemical shifts (δ) were referenced to the residual solvent signals ($CDCl_3$: δH 7.26; δC 77.0). The ^1H NMR spectrum was acquired with 500 scans, relaxation delay (D1) of 1.04 s, and a spectral window of 12 ppm, while the ^{13}C NMR spectrum was obtained with 32,000 scans using broadband proton decoupling (27). Data analysis was performed by combining information from ^1H and ^{13}C NMR (number of atoms, integration, multiplicity, and coupling constants). The presence of methoxy groups was confirmed by proton singlet signals at δH 3.6–3.9 ppm (δC 55–61 ppm). The obtained data were compared with literature values of O-methyl flavonols to confirm the structural assignment.

Molecular docking for anti-inflammatory activity

The potential anti-inflammatory activity of flavonoid compounds was evaluated computationally using molecular docking simulations against several biological targets, namely BTK (PDB ID 3OCS), CASP1 (PDB ID 6PZP), COX-2 (PDB ID 3LN1), IKK (PDB ID 4KIK), INOS (PDB ID 3E7G), JAK2 (PDB ID 4IVA), LOX (PDB ID 6N2W), MPG1 (PDB ID 4AL0), MPO (PDB ID 5QJ2), NOX5 (PDB ID 8U85), PLA2 (PDB ID 5Y5E), and TACE (PDB ID 2OI0). Target structures were obtained from the RCSB Protein Data Bank and prepared by removing water molecules and non-essential ligands, adding polar hydrogen atoms, and assigning Kollman charges using MGLTools v1.5.6 (28).

The flavonoid structures were retrieved from the PubChem database. Reference compounds corresponded to the native ligands extracted directly from the crystallographic structures of each target. All ligand structures were further prepared by adding hydrogen atoms and assigning Gasteiger charges using AutoDock Tools v1.5.6 (29).

Docking simulations were carried out using AutoDock Vina v1.1.2 with default parameters (30). Docking validation was performed by redocking the native ligands into the binding sites of their respective targets, with acceptable reliability criteria referring to RMSD values below 2 Å (31). Binding energies were further analyzed, and molecular interactions between the flavonoid compounds and the targets were visualized using Discovery Studio Visualizer (32).

Pharmacokinetic and toxicity analysis

The pharmacokinetic and toxicity profiles of the flavonol methyl ethers isolated from *A. monopleura* were evaluated using computational approaches. Pharmacokinetic parameters, including absorption, distribution, metabolism, and excretion (ADME), were predicted using the pkCSM platform, which applies graph-based signatures to model compound behavior in biological systems (33). The toxicity of each compound was subsequently assessed using the ProTox 3.0 webserver, which predicts multiple toxicity endpoints through advanced machine-learning algorithms (34).

Results

Extraction

Extraction of *A. monopleura* rhizomes (500 g) using 80% methanol yielded 28.4 g of crude extract with a recovery of 5.7%. The subsequent liquid–liquid partitioning of the methanol extract produced an ethyl acetate fraction weighing 8.7 g, representing 30.6% of the total extract.

Fractionation and purification

The ethyl acetate fraction (8.7 g) was further fractionated using VLC on silica gel 60 GF254 with a stepwise gradient system of n-hexane: ethyl acetate (9:1, 8:2, 7:3, 5:5) and ethyl acetate: methanol (8:2). This process yielded five major fractions with distinct spot profiles. Monitoring of fractions (1 to 5) using n-hexane: ethyl acetate (9:1) as the mobile phase showed that fractions 1 and 2 contained dominant spots with strong fluorescence under UV light at 254 nm, while fractions 3–5 exhibited minor spots with weaker intensity. Visualization with $CeSO_4$–H_2SO_4 reagent revealed yellow–brown and blue–purple spots characteristic of flavonoids (Figure 1A).

Further purification of the dominant fraction (B) using radial chromatography provided sharper and faster separations (Figure 1B), affording two major compounds as pale-yellow solids, each showing a single spot on TLC with n-hexane: ethyl acetate (7:3) as the mobile phase. Compound 2a (42 mg) displayed a yellowish-green visualization, while compound 2b (65 mg) exhibited a blue–purple coloration upon spraying with $CeSO_4$–H_2SO_4 reagent.

Structure elucidation

Isolates 2a and 2b were subsequently characterized using ^1H and ^{13}C NMR spectroscopy (Figures 2-5). Residual $CDCl_3$

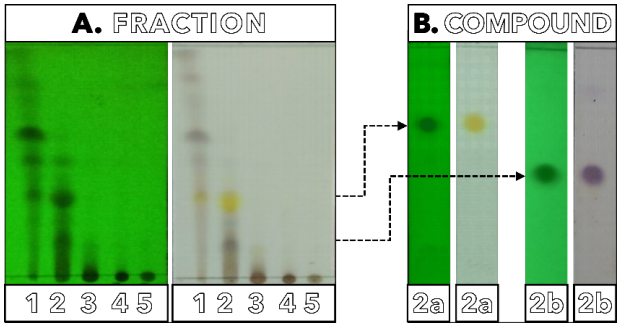

Figure 1. Thin layer chromatography (TLC) profiles of fractionation (A) and compound purification (B) from *Alpinia monopleura* rhizomes with n-hexane: ethyl acetate (9:1), 254 nm and $CeSO_4$–H_2SO_4.

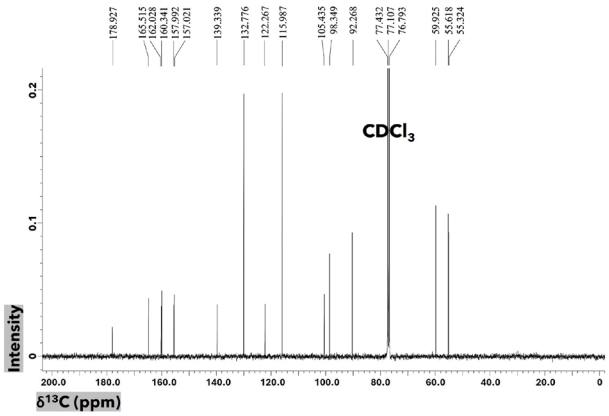

Figure 2. ^{13}C NMR spectrum of compound 2a from *Alpinia monopleura*.

peaks at δH ≈ 7.26 ppm and δC ≈ 77 ppm were clearly observed and did not interfere with the interpretation of core signals. Peak intensity and resolution were sufficient to reliably assign multiplicities and coupling constants (J). Both compounds displayed a carbon resonance at δC ≈ 178.9 ppm, corresponding to the carbonyl carbon (C-4) typical of flavonols. Two meta-coupled aromatic protons on the A-ring (H-6 and H-8) appeared as doublets—compound 2a: δH 6.27 (d, J = 2.0 Hz) and 6.44 (d, J = 2.0 Hz); compound 2b: δH 6.38 (d) and 6.76 (d), confirming a 5,7-dioxygenated substitution pattern.

Both compounds showed three singlet signals at δH 3.82–3.99 ppm and δC 55–60 ppm, corresponding to three methoxy groups. Compound 2a exhibited signals at δH 3.99 (two closely spaced singlets) and 3.93 (singlet), while compound 2b displayed δH 3.94, 3.94, and 3.82 (singlets). These observations indicated the presence of three O-methyl groups, consistent with a trimethyl ether substitution (3,7,4′-O-Me).

The B-ring proton patterns differed between the two compounds. Compound 2a exhibited a para-substituted B-ring pattern with ortho-coupled protons at δH 8.12 (dd, J = 2.4, 8.4 Hz, H-2′,6′) and 7.10 (dd, J = 2.4, 8.4 Hz, H-3′,5′), whereas compound 2b displayed an ABX pattern

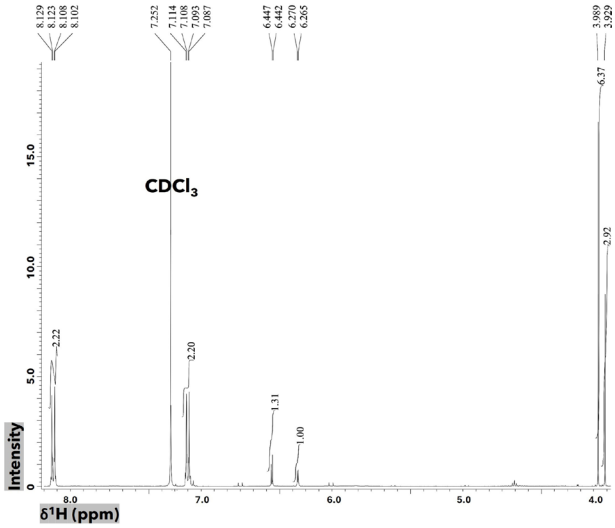

Figure 3. ^{1}H NMR spectrum of compound 2a from *Alpinia monopleura*.

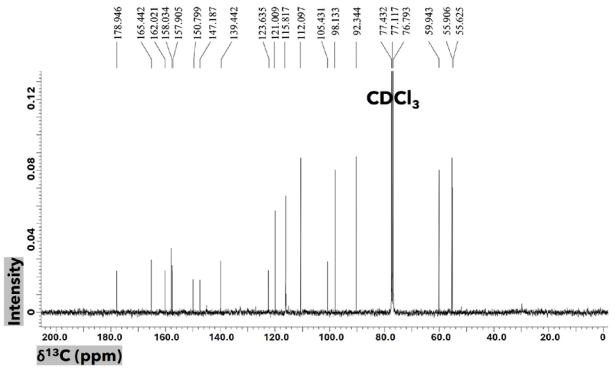

Figure 4. ^{13}C NMR spectrum of compound 2b from *Alpinia monopleura*.

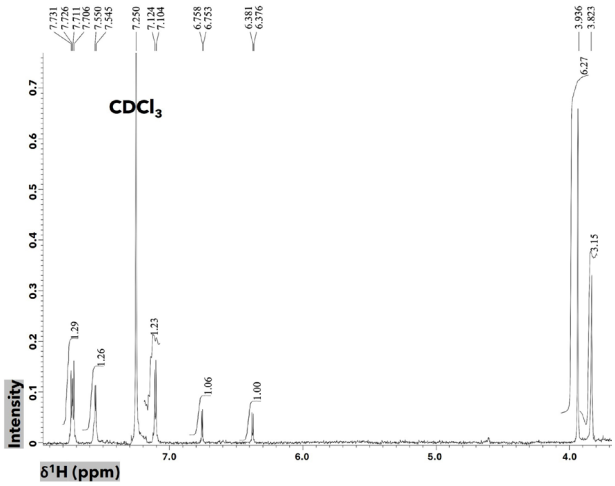

Figure 5. ^{1}H NMR spectrum of compound 2b from *Alpinia monopleura*.

typical of a 1,2,4-trisubstituted ring with δH 7.56 (d, J = 2.0 Hz, H-2′), 7.11 (d, J = 8.0 Hz, H-5′), and 7.72 (dd, J = 2.0, 8.0 Hz, H-6′).

Based on the complete NMR analysis (Tables 1 and

2) and comparison with literature data, compound 2a was identified as kaempferol 3,7,4′-trimethyl ether, and compound 2b as quercetin 3,7,4′-trimethyl ether. The diagnostic evidence supporting these assignments includes the carbonyl signal near δC 178.9 ppm (C-4), the meta-coupled A-ring proton pattern, the presence of three methoxy substituents and distinct B-ring substitution systems corresponding to kaempferol- and quercetin-type skeletons (Figure 6).

Anti-inflammatory activity

Molecular docking analysis was performed to assess the binding profiles of flavonoid compounds 2a and 2b against several protein targets involved in inflammatory pathways. The calculated binding energies for all ligand–protein complexes are summarized in Table 3. In general, more negative binding energy values indicate stronger predicted binding affinity, while values comparable to those of the native ligands suggest similar interaction strength.

Compounds 2a and 2b exhibited more negative binding energies than the native ligands toward iNOS, LOX, and MPG1. For iNOS, both flavonoids showed identical binding energies of -8.5 kcal/mol, which were slightly lower than that of the reference ligand AT2 (-8.2 kcal/mol). For LOX, compound 2a (-7.5 kcal/mol) and

Table 1. NMR data for compound 2a from *Alpinia monopleura* and Kaempferol 3,7,4′-trimethyl ether from the literature

No. C	Compound 2a		Kaempferol 3,7,4′-trimethyl ether (35)	
	δC (ppm)	δH (ppm); ∑H; mult; J (Hz)	δC (ppm)	δH (ppm); ∑H; mult; J (Hz)
2	157.0	-	156.0	-
3	139.3	-	138.9	-
4	178.9	-	178.8	-
4a	105.4	-	106.1	-
5	160.3	-	161.7	-
6	98.3	6.27 (1H, d, 2.0)	97.7	6.34 (1H, d, 2.0)
7	165.5	-	165.4	-
8	92.3	6.44 (1H, d, 2.0)	92.1	6.44 (1H, d, 2.0)
8a	157.9	-	156.7	-
9	59.9	3.99 (3H, s)	59.9	3.84 (3H, s)
10	55.6	3.99 (3H, s)	55.9	3.88 (3H, s)
1′	122.3	-	122.8	-
2′	132.8	8.12 (1H, dd, 2.4 & 8.4)	130.1	8.06 (1H, d, 9.0)
3′	115.9	7.10 (1H, dd, 2.4 & 8.4)	114.0	7.10 (1H, d, 9.0)
4′	162.0	-	162.0	
5′	115.9	7.10 (1H, dd, 2.4 & 8.4)	114.0	7.10 (1H, d, 9.0)
6′	132.8	8.12 (1H, dd, 2.4 & 8.4)	130.1	8.06 (1H, d, 9.0)
7′	55.3	3.93 (3H, s)	55.3	3.86 (3H, s)

Table 2. NMR data for compound 2b from *Alpinia monopleura* and Quercetin 3,7,4′-trimethyl ether from the literature

No C	Compound 2b		Quercetin 3,7,4′-trimethyl ether (36)	
	δC (ppm)	δH (ppm); ∑H; mult; J (Hz)	δC (ppm)	δH (ppm); ∑H; mult; J (Hz)
2	158.0	-	155.4	-
3	139.4	-	138.9	-
4	178.9	-	178.9	-
4a	105.4	-	106.0	-
5	162.0	-	161.9	-
6	98.1	6.38 (1H, d, 2.0)	97.7	6.34 (1H, d, 2.2)
7	165.4	-	165.0	-
8	92.3	6.76 (1H, d, 2.0)	91.9	6.44 (1H, d, 2.2)
8a	157.9	-	156.4	-
9	59.9	3.94 (3H, s)	60.0	3.86 (3H, s)
10	55.9	3.82 (3H, s)	55.6	3.87 (3H, s)
1′	123.6	-	123.5	-
2′	115.8	7.56 (1H, d, 2.0)	114.1	7.69 (1H, d, 2.2)
3′	147.2	-	145.2	-
4′	150.8	-	148.4	-
5′	112.1	7.11 (1H, d, 8.0)	110.4	6.97 (1H, d, 8.6)
6′	121.0	7.72 (1H, dd, 2.0 & 8.0)	121.4	7.72 (1H, dd, 2.2 & 8.6)
7′	55.6	3.94 (3H, s)	55.8	3.96 (3H, s)

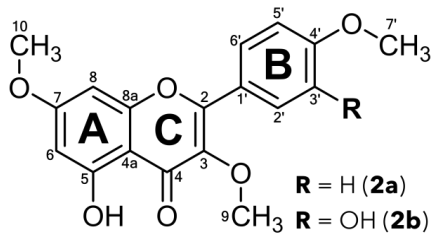

Figure 6. Structures of kaempferol 3,7,4′-trimethyl ether (2a) and quercetin 3,7,4′-trimethyl ether (2b).

compound 2b (-7.2 kcal/mol) displayed binding energies close to that of the control ligand 30Z (-7.1 kcal/mol). In the case of MPG1, compound 2b demonstrated a lower binding energy (-6.3 kcal/mol) compared to compound 2a (-6.0 kcal/mol). Both flavonoids showed more favorable binding energies than the native ligand GSH (-5.4 kcal/mol) at this target.

Analysis of binding interactions revealed that, in the iNOS binding site (Figure 7A-C), compounds 2a and 2b formed hydrogen bonds with Tyr347 and Tyr373. Additional electrostatic interactions were observed with Asp382 for compound 2a and Arg388 for compound 2b. In the LOX complex (Figure 7D-F), both compounds established hydrogen bonds with Gln363 and His432, accompanied by hydrophobic interactions involving Phe359 and Leu368. For MPG1 (Figure 7G-I), the two flavonoids interacted with Arg73, His113, Tyr117, and Arg126, a set of residues that also participate in the binding of the native ligand GSH.

Table 3. Summary of binding energies (kcal/mol) of flavanol methyl ethers against several inflammation-related targets

Targets	Compound 2a	Compound 2b	Native ligand
BTK	-7.7	-7.9	-12.0 (746)
CASP1	-6.3	-6.3	-6.5 (P7S)
COX-2	-9.0	-8.8	-12.3 (celecoxib)
IKK	-8.3	-8.4	-11.8 (KSA)
iNOS	-8.5	-8.5	-8.2 (AT2)
JAK2	-8.1	-8.3	-9.4 (1J5)
LOX	-7.5	-7.2	-7.1 (30Z)
MPG1	-6.0	-6.3	-5.4 (GSH)
MPO	-7.2	-7.2	-7.7 (JXS)
NOX5	-8.4	-8.5	-11.6 (FAD)
PLA2	-7.9	-7.9	-8.8 (7W3)
TACE	-7.8	-8.1	-8.0 (283)

For COX-2, IKK, JAK2, and NOX5, both compounds showed binding energies lower than -8.0 kcal/mol. Among these targets, COX-2 exhibited the most negative binding energies for compounds 2a (-9.0 kcal/mol) and 2b (-8.8 kcal/mol), although these values were still higher than that of the selective inhibitor celecoxib (-12.3 kcal/mol). In the IKK binding site, compounds 2a and 2b showed binding energies of -8.3 and -8.4 kcal/mol, respectively, compared with -11.8 kcal/mol for the native ligand KSA. A comparable binding energy range was observed for JAK2, with values of -8.1 kcal/mol for compound 2a and

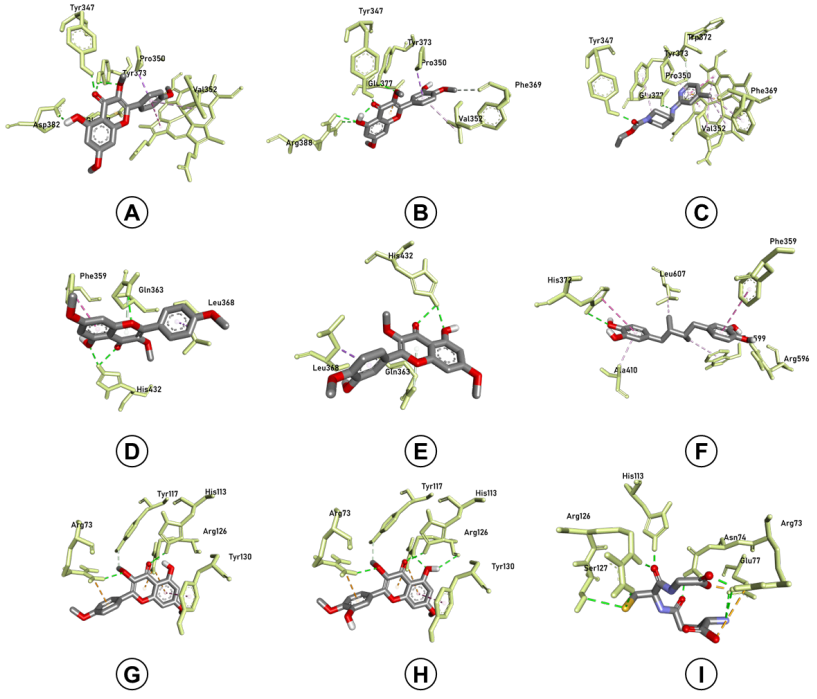

Figure 7. Molecular interactions of flavanol methyl ethers with iNOS, LOX, and mPGES-1. Compound 2a (A), compound 2b (B), and the reference ligand AT2 with inducible nitric oxide synthase (C); compound 2a (D), compound 2b (E), and the reference ligand 30Z with lipoxygenase (F); compound 2a (G), compound 2b (H), and the reference ligand GSH with microsomal prostaglandin E synthase-1 (I).

-8.3 kcal/mol for compound 2b. For NOX5, compound 2a exhibited a binding energy of -8.4 kcal/mol, while compound 2b showed a slightly lower value of -8.5 kcal/mol, compared with -11.6 kcal/mol for the native ligand FAD.

Interaction analysis at the COX-2 active site (Figure 8A-C) indicated that both flavonoids formed hydrogen bonds with Ser339, Phe504, and Ala513, along with hydrophobic interactions involving Val335 and Leu517. These interactions partially overlapped with those observed for celecoxib. However, additional hydrogen bonds with Gln178, Leu338, and Arg499, as well as hydrophobic interactions with Leu370, Tyr371, and Trp373, were only observed in the celecoxib complex.

In the IKK binding site (Figure 8D-F), compounds 2a and 2b displayed similar interaction patterns, forming hydrogen bonds with Asn28, Glu97, and Gly102, and hydrophobic interactions with Leu21, Val29, Ala42, Cys99, Val152, and Ile165. The native ligand KSA shared some of these interactions but additionally formed hydrogen bonds with Gly22 and Glu149, as well as hydrophobic interactions with Lys44 and Met96.

For JAK2 (Figure 8G-I), both flavonoids exhibited comparable binding modes, characterized by hydrogen bonds with Gly856, Glu930, Gly935, and Asn981, and hydrophobic interactions involving Leu855, Val863, Leu983, and Asp994. In contrast, the native ligand 1J5 formed hydrogen bonds with Leu932 and Ser936 and showed overlapping hydrophobic interactions, along with additional contacts involving Ala880, Val911, and Met929. At the NOX5 binding site (Figure 8J-L), compound 2a formed hydrogen bonds with Thr447, Arg463, and Thr548, and hydrophobic interactions with Tyr430, Pro445, and Phe446. Compound 2b exhibited a similar interaction

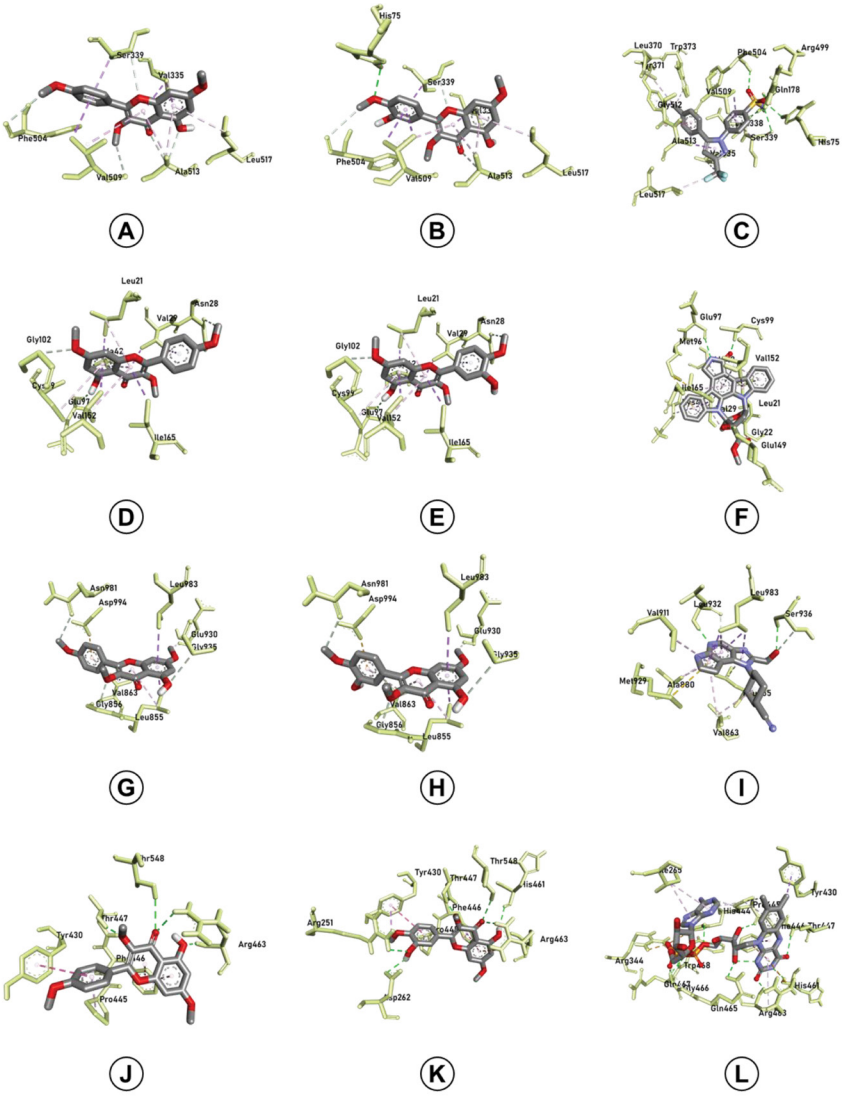

Figure 8. Molecular interactions of flavanol methyl ethers with COX-2, IKK, JAK2, and NOX5. Compound 2a (A), compound 2b (B), and the reference ligand celecoxib with cyclooxygenase-2 (C); compound 2a (D), compound 2b (E), and the reference ligand KSA with IκB kinase (F); compound 2a (G), compound 2b (H), and the reference ligand 1J5 with Janus kinase 2 (I); compound 2a (J), compound 2b (K), and the reference ligand FAD with NADPH oxidase (L).

pattern, with additional hydrogen bonds involving Arg251, Asp262, and His461. The native ligand FAD formed multiple hydrogen bonds with residues Pro445, Thr447, His461, Arg463, Gln465, Gly466, Gln467, and Trp468, as well as hydrophobic interactions with Ile265, Arg344, Tyr430, His444, and Phe446.

Pharmacokinetics profile

The pharmacokinetic characteristics of the flavonol methyl ethers were predicted in silico, as summarized in Table 4. All compounds exhibited high Caco-2 permeability (log Papp > 0.9), indicating strong passive diffusion across the intestinal epithelium and suggesting favorable oral bioavailability. Consistently, intestinal absorption values exceeded 90%, further supporting the likelihood of effective systemic uptake following oral administration.

The flavanols' methyl ethers also showed low steady-state volume of distribution (VDss > –0.15), suggesting limited extravascular distribution and a greater tendency toward plasma retention (33). Both compounds were predicted to inhibit CYP3A4, suggesting potential drug–drug interaction risks through altered metabolic clearance, bioavailability, and half-life of co-administered substrates (37). In addition, the low total systemic clearance values indicate relatively slow elimination, which may contribute to prolonged pharmacological exposure.

Toxicity profile

The predicted toxicity profiles provide important insight into the potential adverse effects of the flavanols methyl ethers, an essential consideration in early drug discovery. Overall, both compounds (2a and 2b) exhibited a generally favorable safety profile, although several organ-specific risks were identified (Table 5). Both compounds were predicted to be non-hepatotoxic, indicating a low likelihood of liver injury. Likewise, predictions for neurotoxicity, cardiotoxicity, mutagenicity, and carcinogenicity were classified as inactive, suggesting minimal risk of central nervous system impairment, cardiac toxicity, genetic damage, or carcinogenic potential. Compound 2a demonstrated a high probability of non-cytotoxicity (0.99), and Compound 2b also showed a low cytotoxicity risk (0.66), supporting their overall cellular safety.

In contrast, both molecules showed active predictions for nephrotoxicity, with moderate probabilities (0.58 for 2a and 0.59 for 2b), indicating a possible risk of kidney-related effects. Respiratory toxicity was also predicted for both compounds (0.73 for 2a and 0.77 for 2b), suggesting a potential impact on respiratory function. Notably, immunotoxicity predictions differed between the two flavanols: Compound 2a was classified as inactive (0.63), whereas Compound 2b exhibited a high probability of immunotoxicity (0.88), indicating potential differences in their immunomodulatory properties.

Discussion

Methanol was chosen as the primary solvent due to its polar and semi-polar nature, which enables the dissolution of a wide range of secondary metabolites,

Table 4. Pharmacokinetics profile of flavanol methyl ethers from *Alpinia monopleura*

Pharmacokinetics profiles	Compound 2a	Compound 2b
Caco2 permeability (log Papp in 10-6 cm/s)	1.161	1.374
Intestinal absorption (% absorbed)	95.355	91.735
Distribution volume (log L/kg)	-0.162	-0.169
CYP2D6 Inhibitor	No	No
CYP3A4 Inhibitor	Yes	Yes
Total clearance (log mL/min/kg)	0.725	0.661

Table 5. Toxicity profile of flavanol methyl ethers from *Alpinia monopleura*

Target	Compound 2a		Compound 2b	
	Prediction	Probability	Prediction	Probability
Hepatotoxicity	Inactive	0.69	Inactive	0.70
Neurotoxicity	Inactive	0.79	Inactive	0.83
Nephrotoxicity	Active	0.58	Active	0.59
Respiratory toxicity	Active	0.73	Active	0.77
Cardiotoxicity	Inactive	0.64	Inactive	0.67
Carcinogenicity	Inactive	0.57	Inactive	0.63
Immunotoxicity	Inactive	0.63	Active	0.88
Mutagenicity	Inactive	0.70	Inactive	0.77
Cytotoxicity	Inactive	0.99	Inactive	0.66

including flavonoids, alkaloids, phenolics, and glycosides. Methanol is also widely employed for the initial extraction of plants from the Zingiberaceae family, as it efficiently extracts both bound and free phenolic compounds (25,38,39). This result indicates that a considerable proportion of the active metabolites was distributed in the medium-polar fraction. Ethyl acetate is known to be selective for flavonoids, particularly in their aglycone form and derivatives, including flavanols methyl ethers, which exhibit low solubility in highly polar solvents but also limited solubility in nonpolar solvents (40,41). These characteristics are consistent with previous reports in *Alpinia* and *Etlingera* species, where ethyl acetate fractions are often enriched in O-methylated flavonoids (42).

VLC was chosen because it enables the separation of compound groups based on polarity with high reproducibility and has been proven effective for isolating flavonoids from plant extracts (43,44). The distinct fluorescence and color reactions observed in the VLC fractions suggest the presence of polyhydroxylated and O-methylated flavonoids, which are commonly found in the *Alpinia* genus. The subsequent radial chromatography step successfully isolated two pure compounds, as indicated by single TLC spots. The differences in spot color yellowish-green for compound 2a and blue–purple for compound 2b are consistent with variations in the number of free hydroxyl groups, supporting the classification of these isolates as O-methylated flavanols. Such compounds are frequently reported in *Alpinia* and *Etlingera* species, which are known for their diverse methylated flavonoid profiles contributing to biological activities such as antioxidant and anti-inflammatory effects (45,46).

NMR spectral interpretation confirmed that both isolated compounds belong to the flavonol subclass of flavonoids, characterized by a C-4 carbonyl and the typical meta-coupled proton pattern on the A-ring (45). The consistent presence of three O-methyl groups indicates extensive methylation, a common modification in *Alpinia* species that enhances compound lipophilicity and influences biological activity (47).

The B-ring substitution pattern provided the key distinction between compounds 2a and 2b. The para-substituted pattern of 2a corresponds to the kaempferol nucleus (4′-hydroxy substitution), while the 1,2,4-trisubstituted pattern of 2b matches the quercetin nucleus (3′,4′-dihydroxy substitution). This differentiation is typical of methoxylated flavonols isolated from members of the Zingiberaceae family, where O-methylation frequently occurs at C-3, C-7, and C-4′ positions (48).

The identification of kaempferol 3,7,4′-trimethyl ether and quercetin 3,7,4′-trimethyl ether in *A. monopleura* adds to the growing evidence that this genus is a rich source of O-methylated flavonoids. These compounds are often associated with strong antioxidant, anti-inflammatory, and anticancer properties due to their structural balance between hydrophobic methoxy groups and hydrophilic hydroxyl sites (45,49).

This study explores the molecular basis underlying the anti-inflammatory potential of kaempferol 3,7,4′-trimethyl ether (2a) and quercetin 3,7,4′-trimethyl ether (2b), two O-methylated flavonols derived from *A. monopleura*, using a multi-target docking strategy. The computational findings delineate interaction patterns that may explain how structural variations among methylated flavonoids influence their engagement with inflammatory regulators. A central structural feature influencing the interactions of both compounds is O-methylation of the flavonol scaffold. In compound 2a, the reduced hydroxylation pattern on the B-ring shifts the electronic distribution toward a more hydrophobic and conformationally rigid scaffold (50). Such structural characteristics are consistent with COX-2 recognition, given the predominance of hydrophobic contacts within the COX binding pocket. This observation is aligned with previous reports indicating that methylated kaempferol analogues exhibit enhanced COX-2 selectivity through strengthened hydrophobic interactions, including π–π stacking and van der Waals contacts (21). In addition, reported anti-inflammatory mechanisms of kaempferol, such as suppression of NF-κB signaling and modulation of upstream kinases including Src, Syk, IRAK1, and IRAK4, further support the relevance of the computational predictions (51).

In contrast, compound 2b retains a higher degree of polarity due to its quercetin-derived B-ring substitution pattern (52). The presence of additional hydroxyl groups facilitates a more diverse hydrogen-bonding network, which may favor interactions with kinase-associated and redox-sensitive targets (53). This structural characteristic provides a plausible explanation for its predicted affinity toward signaling hubs such as IKK and JAK2, which play central roles in coordinating NF-κB and JAK/STAT-mediated inflammatory responses (54,55). Moreover, the interaction of compound 2b with enzymes involved in reactive oxygen and nitrogen species production supports the notion that quercetin methyl ethers may influence inflammatory processes at both transcriptional and oxidative levels (56).

The multi-target interaction patterns observed for both compounds are consistent with previous reports on methylated flavonoids isolated from *Alpinia* species, including kaempferide, isorhamnetin, and methoxygalangin derivatives, which have demonstrated broad bioactivity against inflammation, hyperlipidemia, and cancer (57,58). In addition, kaempferol has been reported to exhibit anti-inflammatory effects across various disease models, including atherosclerosis, osteoarthritis, and colitis (59-61). The in silico pharmacokinetic assessment suggests that both compounds possess physicochemical properties compatible with oral administration, including favorable intestinal absorption and membrane permeability. At the same time, although the predicted toxicological profiles were generally

favorable, these findings still warrant careful experimental validation.

Overall, this computational investigation provides a mechanistic framework suggesting that kaempferol 3,7,4′-trimethyl ether and quercetin 3,7,4′-trimethyl ether may engage multiple nodes within inflammatory signaling networks. However, as these findings are derived from docking-based simulations, further experimental studies are required to confirm their biological activities and to assess their therapeutic feasibility as anti-inflammatory agents.

Conclusion

In this study, phytochemical investigation of *A. monopleura* led to the isolation and structural identification of two O-methylated flavonols, kaempferol 3,7,4′-trimethyl ether (2a) and quercetin 3,7,4′-trimethyl ether (2b). Using a multi-target in silico approach, these compounds were suggested to possess potential anti-inflammatory activity. Both flavonols were predicted to interact with several key proteins involved in inflammatory signaling and mediator synthesis, including pathways associated with prostaglandin production, cytokine regulation, nitric oxide generation, and oxidative stress.

In silico pharmacokinetic and toxicity predictions indicated physicochemical properties compatible with oral administration and generally acceptable safety profiles, supporting their suitability for further investigation. However, as the present findings are derived exclusively from computational analyses, comprehensive in vitro validation is required to confirm the predicted pharmacological activities of these flavonol methyl ethers.

Acknowledgement

The authors express their sincere appreciation to Politeknik Bina Husada Kendari and Universitas Halu Oleo for providing the facilities that supported the implementation of this research. The authors also extend their gratitude to the National Research and Innovation Agency, Indonesia, for its assistance in conducting NMR measurements.

Authors' contribution

Conceptualization: Agung Wibawa Mahatva Yodha and Wahyuni
Data curation: Agung Wibawa and Reymon.
Formal analysis: Angriani Fusvita and Wahyuni.
Funding acquisition: Agung Wibawa Mahatva Yodha.
Investigation: Wahyuni and Nirwati Rusli.
Methodology: Musdalipah and Sahidin.
Project administration: Reymon and Nirwati Rusli.
Resources: Wahyuni and Musdalipah.
Software: Arfan.
Supervision: Sahidin.
Validation: Arfan and Sahidin.
Visualization: Arfan and Wahyuni.
Writing–original draft: Agung Wibawa Mahatva Yodha.
Writing–review & editing: All authors.

Conflict of interests

The authors declare that they have no known conflicts of interest that could have influenced the work reported in this paper.

Declaration of AI-assisted tools in the writing procedure

The authors used ChatGPT (OpenAI, USA) and DeepL Translator (DeepL Agent, Germany) for language editing and grammatical refinement. All AI-assisted content was carefully reviewed and approved by the authors to ensure the accuracy and integrity of the scientific content.

Ethical considerations

This research does not involve animals or humans in the experiment.

Funding/Support

This work was supported by the Ministry of Higher Education, Science and Technology of the Republic of Indonesia through the Fundamental Research Grant under Contract No. 205/C3/DT.05.00/PL-BATCH II/2025

References

1. Sheikh AM, Yano S, Tabassum S, Nagai A. The role of the vascular system in degenerative diseases: Mechanisms and implications. Int J Mol Sci. 2024;25(4):2169. doi:10.3390/ijms25042169
2. Yacine A, Zain Ali M, Alharbi AB, Qubayl Alanaz H, Saud Alrahili A, Alkhdairi AA. Chronic inflammation: A multidisciplinary analysis of shared pathways in autoimmune, infectious, and degenerative diseases. Cureus. 2025;17(4):e82579. doi:10.7759/CUREUS.82579
3. Gopalan C, Kirk E. Inflammation. Biol Cardiovasc Metab Dis. 2022;53–66. doi:10.1016/B978-0-12-823421-1.00014-7
4. Herrera TES, Tello IPS, Mustafa MA, Jamil NY, Alaraj M, Atiyah Altameem KK, et al. Kaempferol: Unveiling its anti-inflammatory properties for therapeutic innovation. Cytokine. 2025;186:156846. doi:10.1016/J.CYTO.2024.156846
5. Metkin G, Süntar İ, Şenol Deniz FS, Tugay O, Demiralp M, Pittalà V. Investigating COX-2 and 5-LOX enzyme-related anti-inflammatory and antioxidant activities and phytochemical features of *Scutellaria salviifolia* Benth. Int J Mol Sci. 2025;26(12):5608. doi:10.3390/ijms26125608
6. Lim HJ, Prajapati R, Seong SH, Jung HA, Choi JS. Antioxidant and antineuroinflammatory mechanisms of kaempferol-3-O-β-d-glucuronate on lipopolysaccharide-stimulated BV2 microglial cells through the Nrf2/HO-1 signaling cascade and MAPK/NF-κB Pathway. ACS Omega. 2023;8(7):6538–49. doi:10.1021/ACSOMEGA.2C06916
7. Xiong G, Ji W, Wang F, Zhang F, Xue P, Cheng M, et al. Quercetin inhibits inflammatory response induced by LPS from *Porphyromonas gingivalis* in human gingival fibroblasts via suppressing NF-κB signaling pathway. Biomed Res Int. 2019;2019(1):6282635. doi:10.1155/2019/6282635
8. Kravchenko I, Eberle L, Nesterkina M, Kobernik A. Anti-inflammatory and analgesic activity of ointment based on dense ginger extract (*Zingiber officinale*). J Herbmed

Pharmacol. 2019;8(2):126–32. doi:10.15171/JHP.2019.20
9. Khairullah AR, Solikhah TI, Ansori ANM, Hanisia RH, Puspitarani GA, Fadholly A, et al. Medicinal importance of *Kaempferia galanga* L. (Zingiberaceae): A comprehensive review. J Herbmed Pharmacol. 2021;10(3):281–8. doi:10.34172/JHP.2021.32
10. Karmilah K, Yodha AWM, Hamsidi R, Daud NS, Malaka MH, Musdalipah M, et al. Antioxidant and anti-inflammatory activities of diarylheptanoid from *Etlingera calophrys* fruit. Molekul. 2024;19(3):604–13. doi:10.20884/1.JM.2024.19.3.12413
11. Jabbar A, Yusuf MI, Wahyuni, Hamzah H, Windarsih A, Pratiwi SUT, et al. LC-MS analysis, antioxidant and anti-inflamatory activity, isolation of secondary metabolite of ethanol extract stem of *Etlingera rubroloba* AD Poulsen. Case Stud Chem Environ Eng. 2024;10:100780. doi:10.1016/J.CSCEE.2024.100780
12. Hamsidi R, Wahyuni W, Sahidin I, Apriyani E, Harsono H, Azizah NA, et al. Suppression of proinflammatory cytokines by *Etlingera alba* (A.D.) Poulsen rhizome extract and its antibacterial properties. Adv Pharmacol Pharm Sci. 2021;2021(1):5570073. doi:10.1155/2021/5570073
13. Yodha AWM, Badia E, Musdalipah, Reymon, Fauziah Y, Fusvita A, et al. Secondary metabolite compounds from *Alpinia monopleura* extract and evaluation of anti-inflammatory activity based on in vitro and in silico studies. HAYATI J Biosci. 2024;31(6):1154–64. doi:10.4308/hjb.31.6.1154-1164
14. Zohmachhuana A, Kumar NS, Malsawmdawngliana, Mathipi V, Lalrinzuali, Parimelazhagan T, et al. *Alpinia galanga* induces caspase-dependent apoptotic cell death in human lung and cervical cancer cells. J Herbmed Pharmacol. 2024;13(4):640–50. doi:10.34172/JHP.2024.52571
15. Yuliawati KM, Febriyanti RM, Sumiwi SA, Levita J. Anti-inflammatory activities of some plants of genus *Alpinia*: Insights from in vitro, in vivo, and human studies. J Exp Pharmacol. 2025;17:51–91. doi:10.2147/JEP.S499115
16. Yodha AWM, Badia E, Musdalipah, Setiawan MA, Daud NS, Fusvita A, et al. Essential oils of *Alpinia monopleura* and their antibacterial and antioxidant activity. Molekul. 2023;18(1):80–8. doi:10.20884/1.JM.2023.18.1.6265
17. Wahyuni W, Fristiohadi A, Sahidin I, Yodha AWM, Purnama LOMJ, Idrus LS, et al. Identification of potential anticancer bioactive compounds from fractions of A*lpinia monopleura* rhizome extract. Pakistan J Biol Sci. 2025;28(4):253–66. doi:10.3923/PJBS.2025.253.266
18. Walle T. Methylation of dietary flavones increases their metabolic stability and chemopreventive effects. Int J Mol Sci. 2009;10(11):5002–19. doi:10.3390/IJMS10115002
19. Yang JH, Kim SC, Shin BY, Jin SH, Jo MJ, Jegal KH, et al. O-methylated flavonol isorhamnetin prevents acute inflammation through blocking of NF-κB activation. Food Chem Toxicol. 2013;59:362–72. doi:10.1016/J.FCT.2013.05.049
20. Zhong R, Miao L, Zhang H, Tan L, Zhao Y, Tu Y, et al. Anti-inflammatory activity of flavonols via inhibiting MAPK and NF-κB signaling pathways in RAW264.7 macrophages. Curr Res Food Sci. 2022;5:1176. doi:10.1016/J.CRFS.2022.07.007
21. Md Idris MH, Mohd Amin SN, Mohd Amin SN, Nyokat N, Khong HY, Selvaraj M, et al. Flavonoids as dual inhibitors of cyclooxygenase-2 (COX-2) and 5-lipoxygenase (5-LOX): Molecular docking and in vitro studies. Beni-Suef Univ J Basic Appl Sci. 2022;11(1):117. doi:10.1186/s43088-022-00296-y
22. Gong G, Guan YY, Zhang ZL, Rahman K, Wang SJ, Zhou S, et al. Isorhamnetin: A review of pharmacological effects. Biomed Pharmacother. 2020;128:110301. doi:10.1016/J.BIOPHA.2020.110301
23. Tang S, Wang B, Liu X, Xi W, Yue Y, Tan X, et al. Structural insights and biological activities of flavonoids: Implications for novel applications. Food Front. 2025;6(1):218–47. doi:10.1002/FFT2.494
24. Bitwell C, Indra S Sen, Luke C, Kakoma MK. A review of modern and conventional extraction techniques and their applications for extracting phytochemicals from plants. Sci African. 2023;19:e01585. doi:10.1016/J.SCIAF.2023.E01585
25. Wu D, Ge D, Dai Y, Chen Y, Fu Q, Jin Y. Extraction and isolation of diphenylheptanes and flavonoids from *Alpinia officinarum* Hance using supercritical fluid extraction followed by supercritical fluid chromatography. J Sep Sci. 2023;46(14):2300156. doi:10.1002/JSSC.202300156
26. Nkwocha CC, Felix JO, Michael LO, Ale BA. Phytochemical screening and GC-FID identification of bioactive compounds in n-hexane, ethylacetate and methanol fractions of methanolic leaves extract of *Azanza garckeana*. Food Chem Adv. 2024;4:100712. doi:10.1016/J.FOCHA.2024.100712
27. Janovick J, Spyros A, Dais P, Hatzakis E. Nuclear magnetic resonance. Chem Anal Food Tech Appl Second Ed. 2020;135–75. doi:10.1016/B978-0-12-813266-1.00004-8
28. Morris GM, Huey R, Lindstrom W, Sanner MF, Belew RK, Goodsell DS, et al. AutoDock4 and AutoDockTools4: Automated docking with selective receptor flexibility. J Comput Chem. 2009;30(16):2785–91. doi:10.1002/jcc.21256
29. Arfan A, Rayani N, Ruslin R, Kasmawati H, Aman LO, Asnawi A. Rigid and flexible docking study with ADME evaluation of hesperetin analogs as LecB inhibitors in *Pseudomonas aeruginosa*. Indones J Pharm Sci Technol. 2024;6(2):15–25. doi:10.24198/ijpst.v6i2.52623
30. Trott O, Olson AJ. AutoDock Vina: Improving the speed and accuracy of docking with a new scoring function, efficient optimization, and multithreading. J Comput Chem. 2010;31(2):455–61. doi:10.1002/JCC.21334
31. Arfan A, Asnawi A, Aman LO. Marine sponge Xestospongia sp.: A promising source for tuberculosis drug development - computational insights into mycobactin biosynthesis inhibition. Borneo J Pharm. 2024;7(1):40–50. doi:10.33084/BJOP.V7I1.5513
32. Arfan A, Ruslin R, Yamin Y, Annisa F, Basrin WOF. Exploring the anti-inflammatory activity of purified *Ficus septica* extracts: Insights from in vitro and in silico studies. J Sains Farm Klin. 2025;11(3):189–96. doi:10.25077/jsfk.11.3.189-196.2024
33. Pires DEV, Blundell TL, Ascher DB. pkCSM: Predicting small-molecule pharmacokinetic and toxicity properties using graph-based signatures. J Med Chem. 2015;58(9):4066–72. doi:10.1021/acs.jmedchem.5b00104
34. Banerjee P, Kemmler E, Dunkel M, Preissner R. ProTox 3.0: A webserver for the prediction of toxicity of chemicals. Nucleic Acids Res. 2024;52(1):513–20. doi:10.1093/nar/gkae303
35. Hung HD, Tien DD, Ngoan NT, Duong BT, Viet DQ, Dien PG, et al. Chemical constituents from the leaves of *Terminalia catappa* L. (Combretaceae). Vietnam J Sci Technol. 2022;60(4):625–30. doi:10.15625/2525-2518/15972
36. Silva JI de M, Scheffer MC, Lima LM, Nunez CV. Antibacterial activity of Vitex cymosa extracts and identification of ayanin. Rev Bras Plantas Med. 2025;27(2025):e2025003–e2025003. doi:10.70151/34MTTT61

37. Klyushova LS, Perepechaeva ML, Grishanova AY. The role of CYP3A in health and disease. Biomedicines. 2022; 10(11):1–52. doi:10.3390/biomedicines10112686
38. Haroen U, Syafwan S, Kurniawan K, Budiansyah A. Determination of total phenolics, flavonoids, and testing of antioxidant and antibacterial activities of red ginger (*Zingiber officinale* var. Rubrum). J Adv Vet Anim Res. 2024;11(1):114. doi:10.5455/JAVAR.2024.K755
39. Geraldi A, Manuhara YSW, Wibowo AT, Wardana AP, Aminah NS, Kristanti AN, et al. Methanolic extracts of Zingiberaceae family plants from Indonesia as antibacterial agents. J Med Pharm Chem Res. 2025;7(12):2743–54. doi:10.48309/JMPCR.2025.507161.1603
40. Rodríguez De Luna SL, Ramírez-Garza RE, Serna Saldívar SO. Environmentally friendly methods for flavonoid extraction from plant material: Impact of their operating conditions on yield and antioxidant properties. Sci World J. 2020;2020:6792069. doi:10.1155/2020/6792069
41. Esati NK, La EOJ, Sudiasih NP, Saniasih NND. Total flavonoid levels in n-hexane and ethyl acetate fractions of *Rosmarinus officinalis* L. leaves and their antibacterial and antioxidant activities. Borneo J Pharm. 2024;7(1):51–62. doi:10.33084/BJOP.V7I1.4034
42. Aziz IM, Alfuraydi AA, Almarfadi OM, Aboul-Soud MAM, Alshememry AK, Alsaleh AN, et al. Phytochemical analysis, antioxidant, anticancer, and antibacterial potential of *Alpinia galanga* (L.) rhizome. Heliyon. 2024;10(17):e37196. doi:10.1016/J.HELIYON.2024.E37196
43. Sharma A, Kathuria D, Kolita B, Gohain A, Das AK, Bhardwaj G, et al. Greener approach for the isolation of oleanolic acid from *Nepeta leucophylla* Benth. Its derivatization and their molecular docking as antibacterial and antiviral agents. Heliyon. 2023;9(8):e18639. doi:10.1016/J.HELIYON.2023.E18639
44. Rahmawati R, Hartati YW, Latip J binti, Herlina T. An overview of techniques and strategies for isolation of flavonoids from the genus *Erythrina*. J Sep Sci. 2023; 46(12):2200800. doi:10.1002/JSSC.202200800
45. Koirala N, Thuan NH, Ghimire GP, Thang D Van, Sohng JK. Methylation of flavonoids: Chemical structures, bioactivities, progress and perspectives for biotechnological production. Enzyme Microb Technol. 2016;86:103–16. doi:10.1016/J.ENZMICTEC.2016.02.003
46. Mayasari D, Murti YB, Pratiwi SUT, Sudarsono. Antibacterial activity and TLC-densitometric analysis of secondary metabolites in the leaves of the traditional herb, *Melastoma malabathricum* L. Borneo J Pharm. 2022; 5(4):334–44. doi:10.33084/BJOP.V5I4.3818
47. Ma XN, Xie CL, Miao Z, Yang Q, Yang XW. An overview of chemical constituents from *Alpinia* species in the last six decades. RSC Adv. 2017;7(23):14114–44. doi:10.1039/C6RA27830B
48. Liu Y, Fernie AR, Tohge T. Diversification of chemical structures of methoxylated flavonoids and genes encoding flavonoid-O-methyltransferases. Plants. 2022;11(4):564. doi:10.3390/PLANTS11040564
49. Ullah A, Munir S, Badshah SL, Khan N, Ghani L, Poulson BG, et al. Important flavonoids and their role as a therapeutic agent. Molecules. 2020;25(22):5243. doi:10.3390/MOLECULES25225243
50. Sengupta B, Biswas P, Roy D, Lovett J, Simington L, Fry DR, et al. Anticancer properties of kaempferol on cellular signaling pathways. Curr Top Med Chem. 2022;22(30):2474–82. doi:10.2174/1568026622666220907112822
51. Kim SH, Park JG, Lee J, Yang WS, Park GW, Kim HG, et al. The dietary flavonoid Kaempferol mediates anti-inflammatory responses via the Src, Syk, IRAK1, and IRAK4 molecular targets. Mediators Inflamm. 2015;2015(1):1–15. doi:10.1155/2015/904142
52. Safna HKP, Davis A, Lekshmi S, Thayyil MS, Raghavamenon AC, Babu TD. Evaluation of the binding efficacy of flavonol derivatives on estrogen receptors (ER) with respect to ring B hydroxylation. Results Chem. 2024;7:1–13. doi:10.1016/j.rechem.2024.101544
53. Kongpichitchoke T, Hsu JL, Huang TC. Number of hydroxyl groups on the B-ring of flavonoids affects their antioxidant activity and interaction with phorbol ester binding site of PKCδ C1B domain: In vitro and in silico studies. J Agric Food Chem. 2015;63(18):4580–6. doi:10.1021/acs.jafc.5b00312
54. Mao H, Zhao X, Sun S cong. NF-κB in inflammation and cancer. Cell Mol Immunol. 2025;22(8):811–39. doi:10.1038/s41423-025-01310-w
55. Sarapultsev A, Gusev E, Komelkova M, Utepova I, Luo S, Hu D. JAK-STAT signaling in inflammation and stress-related diseases: Implications for therapeutic interventions. Mol Biomed. 2023;4(1):40. doi:10.1186/s43556-023-00151-1
56. Mahat MYA, Kulkarni NM, Vishwakarma SL, Khan FR, Thippeswamy BS, Hebballi V, et al. Modulation of the cyclooxygenase pathway via inhibition of nitric oxide production contributes to the anti-inflammatory activity of kaempferol. Eur J Pharmacol. 2010;642(1–3):169–76. doi:10.1016/j.ejphar.2010.05.062
57. Nishidono Y, Tanaka K. Phytochemicals of Alpinia zerumbet: A review. Molecules. 2024;29(12):1–24. doi:10.3390/molecules29122845
58. Youn I, Han AR, Piao D, Lee H, Kwak H, Lee Y, et al. Phytochemical and pharmacological properties of the genus *Alpinia* from 2016 to 2023. Nat Prod Rep. 2024;41(9):1346–67. doi:10.1039/D4NP00004H
59. Park MY, Ji GE, Sung MK. Dietary kaempferol suppresses inflammation of dextran sulfate sodium-induced colitis in mice. Dig Dis Sci. 2012;57(2):355–63. doi:10.1007/s10620-011-1883-8
60. Zhuang Z, Ye G, Huang B. Kaempferol alleviates the interleukin-1β-induced inflammation in rat osteoarthritis chondrocytes via suppression of NF-κB. Med Sci Monit. 2017;23:3925-31. doi:10.12659/msm.902491
61. Kong L, Luo C, Li X, Zhou Y, He H. The anti-inflammatory effect of kaempferol on early atherosclerosis in high cholesterolfed rabbits. Lipids Health Dis. 2013;12(1):115. doi:10.1186/1476-511X-12-115